

Simultaneous Induction of High Level Thermo- and Visible Light-Catalytic Activities to Titanium(IV) Oxide by Surface Modification with Cobalt(III) Oxide Clusters

Qiliang Jin, Hironori Yamamoto, Kotaro Yamamoto, Musashi Fujishima, and Hiroaki Tada *

Department of Applied Chemistry, School of Science and Engineering, Kinki University, 3-4-1, Kowakae, Higashi-Osaka, Osaka 577-8502, Japan

Experimental

Conversion of 2-naphthol to CO₂: In both the thermocatalytic and photocatalytic reactions, TiO₂ or Co₂O₃/TiO₂ (0.25 g) was added to an aqueous solution of 1 mmol dm⁻³ 2-naphthol (10 mL). The suspension was placed in a glass test tube (30 mL). In the dark reaction, the temperature was maintained at 323 K. In the photocatalytic reaction, the test tube was irradiated with a Xe lamp (Wacom XRD-501SW) through a high pass filter (L-42, Toshiba) to cut off UV-light ($I_{420-480\text{ nm}} = 4.0\text{ mW cm}^{-2}$) at 298 K. The CO₂ dissolved in the solution was liberated into the gas phase by adding 0.1 mL sulfuric acid, and then the amount of CO₂ was quantified by gas chromatography (GC-2014, Shimadzu) with methanizer (MTN-1, Shimadzu) [measurement conditions: column = Porapak-Q 80-100 (GL science); N₂ flow rate = 50 mL min⁻¹].

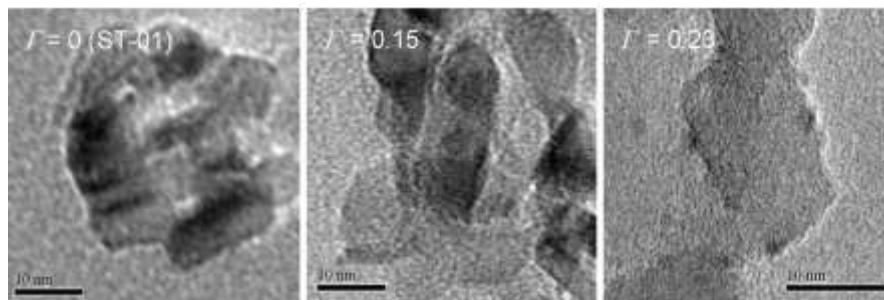


Fig. S1 TEM images of Co₂O₃/TiO₂ with $\Gamma = 0, 0.15,$ and $0.23.$

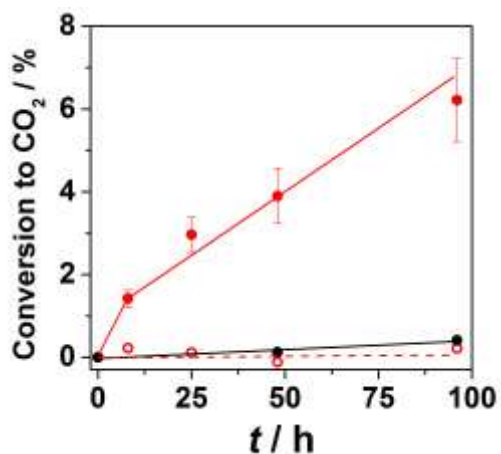


Fig. S2 Time courses for the CO₂ generation in the thermocatalytic reaction in the dark at 323 K in the presence of Co₂O₃($\Gamma = 0.17$)/TiO₂ with (red solid circle) and without (red open circle) 2-naphthol, and in the presence of TiO₂ with 2-naphthol (black solid circle).

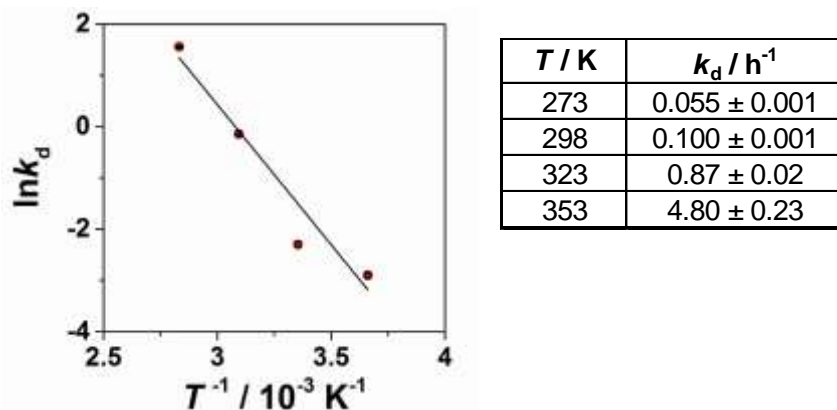


Fig. S3 Arrhenius plot for the $\text{Co}_2\text{O}_3(\Gamma = 0.17)/\text{TiO}_2$ -thermocatalyzed degradation of 2-naphthol (left), and numerical values are shown in the right table.

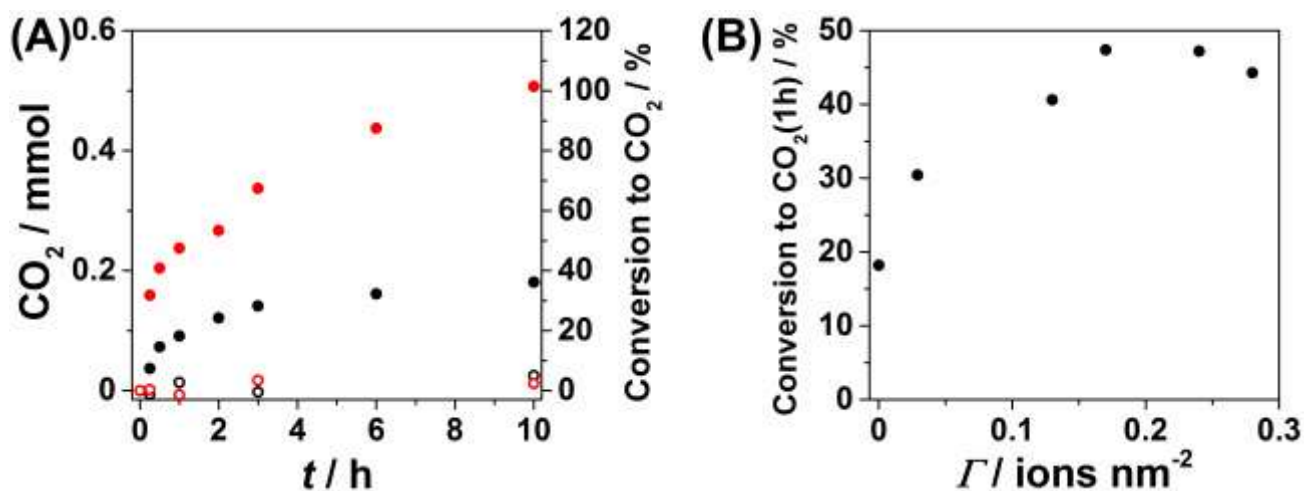


Fig. S4 (A) Time courses for the CO_2 generation in the thermocatalytic degradation of formic acid in the dark at 323 K in the presence of TiO_2 (black solid circle) and $\text{Co}_2\text{O}_3(\Gamma = 0.17)/\text{TiO}_2$ (red solid circle), and in the presence of TiO_2 (black open circle) and $\text{Co}_2\text{O}_3(\Gamma = 0.17)/\text{TiO}_2$ (red open circle) without formic acid. (B) Plots of conversion to CO_2 at 1 h vs. Γ .

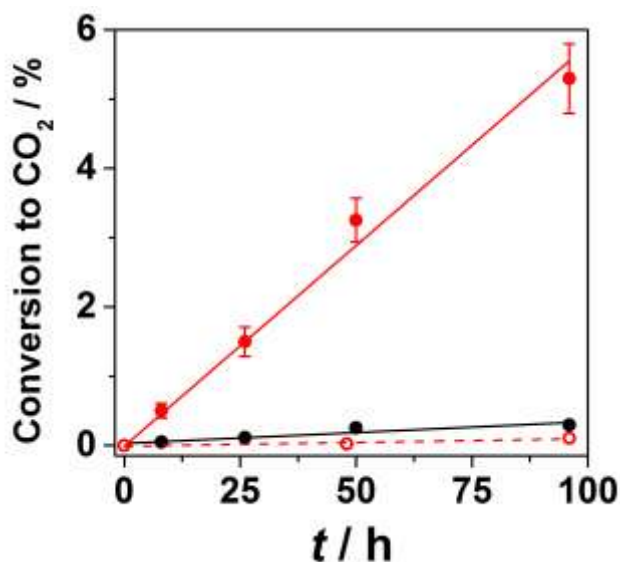


Fig. S5 Time courses for the CO₂ generation in the 2-naphthol degradation under visible-light irradiation at 298 K in the presence of TiO₂ (black solid circle) and Co₂O₃($\Gamma = 0.17$)/TiO₂ (red solid circle). Plot (red open circle) is the data for Co₂O₃($\Gamma = 0.17$)/TiO₂ without 2-naphthol.

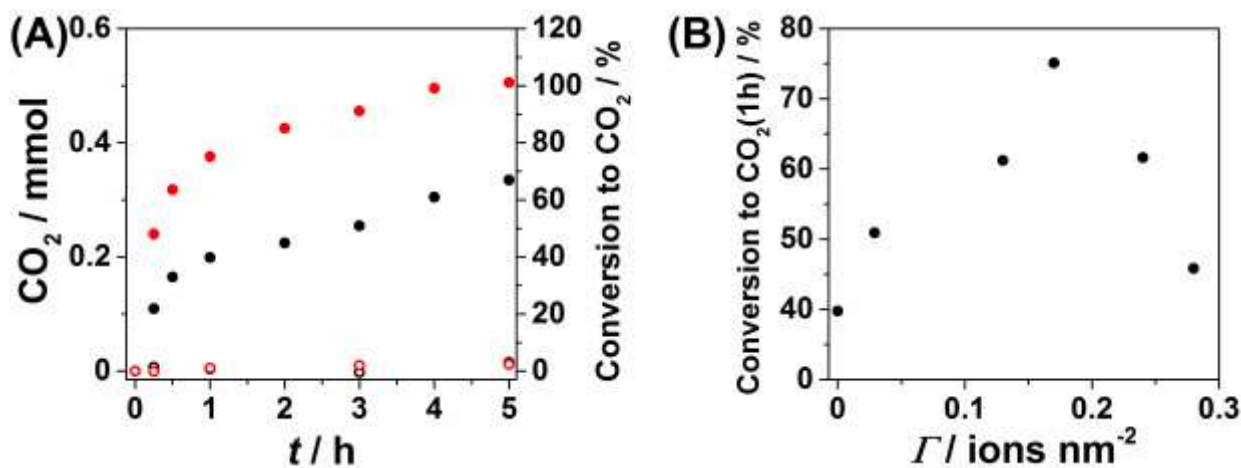


Fig. S6 (A) Time courses for the CO₂ generation in the degradation of formic acid under visible-light irradiation at 298 K in the presence of TiO₂ (black solid circle) and Co₂O₃($\Gamma = 0.17$)/TiO₂ (red solid circle), and in the presence of TiO₂ (black open circle) and Co₂O₃($\Gamma = 0.17$)/TiO₂ (red open circle) without formic acid. (B) Plots of conversion to CO₂ at 1 h vs. Γ .

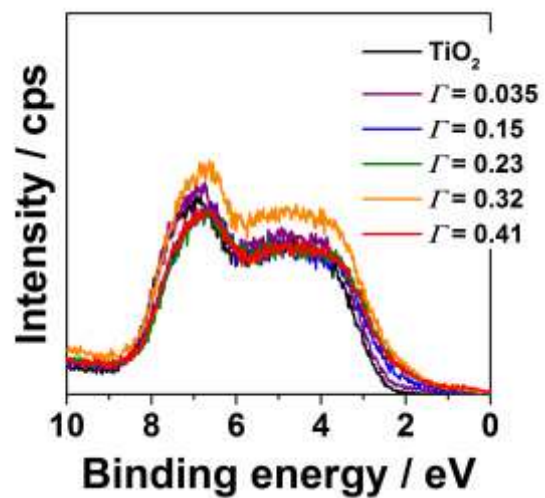


Fig. S7 Valence-band XPS spectra for $\text{Co}_2\text{O}_3/\text{TiO}_2$ with varying Γ .

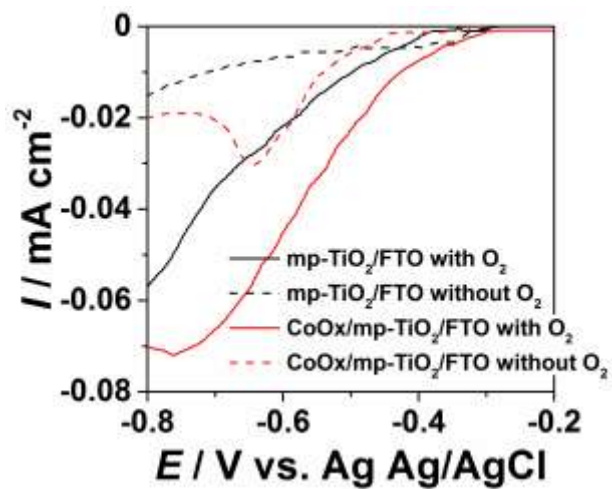


Fig. S8 Current (I/mA)-potential (E/V vs. Ag/AgCl) curves of the mp-TiO₂/FTO electrodes with and without the Co₂O₃-surface modification in a 0.1 mol dm⁻³ NaClO₄ aqueous solution in the dark.